J.Sci.Soc.Thailand, 23(1997) 259-280

REVIEW ARTICLE

A REVIEW OF EXTRUDATE SWELL IN POLYMERS

C. SIRISINHA

Department of Chemistry, Faculty of Science, Mahidol University, Rama 6 Rd., Bangkok 10400, Thailand.

(Received 22 July, 1997)

1. INTRODUCTION

Extrusion is a process which forces polymer melt through a nozzle or die to give a profiled strip of material called an extrudate. Ideally, rubber extrudates which are required for sub-components and end products, including tyre treads, hoses and profiles as well as electrical cables and wires, must have minimum variation in dimensions. This variation is related to the increase in cross-sectional area of the extrudate (swell) after emerging from the die exit.

It can be seen that extrudate swell (also known as die swell) is one of the most crucial factors which affect the cross-sectional dimensions and shape of extrudates in the rubber extrusion process. As a consequence, understanding the factors which control extrudate swell is important for extrusion processes and is the objective of this review.

The review provides details of the factors which govern extrudate swell and the measurement of extrudate swell, including the calculations of recoverable strain and relaxation time based on the Maxwell model. In addition, the influence of fillers on extrudate swell is considered; in particular, the influence of filler dispersion, based on the release of immobilised rubber as filler dispersion increases. This review also includes the origins of wall slip, rubber-carbon black tridimensional transient network and their influences on extrudate swell.

Basically, extrudate swell is controlled by melt elasticity and therefore depends on factors such as temperature, shear stress, shear rate, die geometry, molecular characteristics and filler loading.

Leblanc[1] reviewed five major regions in a die, as shown in Fig. 1:

i) Entrance region

In the die entrance region, elongational flow is dominant and is less pronounced in converging-entry dies than in flat or plate dies, because of the lower extent of molecular deformation at the entrance region in converging dies. Furthermore, the converging-entry die reduces the problem of a stagnant region (the so-called dead spot), which can cause problems of scorch (premature vulcanisation) or molecular degradation in the corners of the entrance region.

ii) Relaxation region

In this region, the stressed molecules dissipate their stored elastic energy caused by elongational flow from σ_0 at the die entrance to σ_t at the die exit, because of Brownian motion. As a result, the entrance effect on extrudate swell will disappear if the relaxation region of the die is sufficiently long (Figs. 2 and 3).

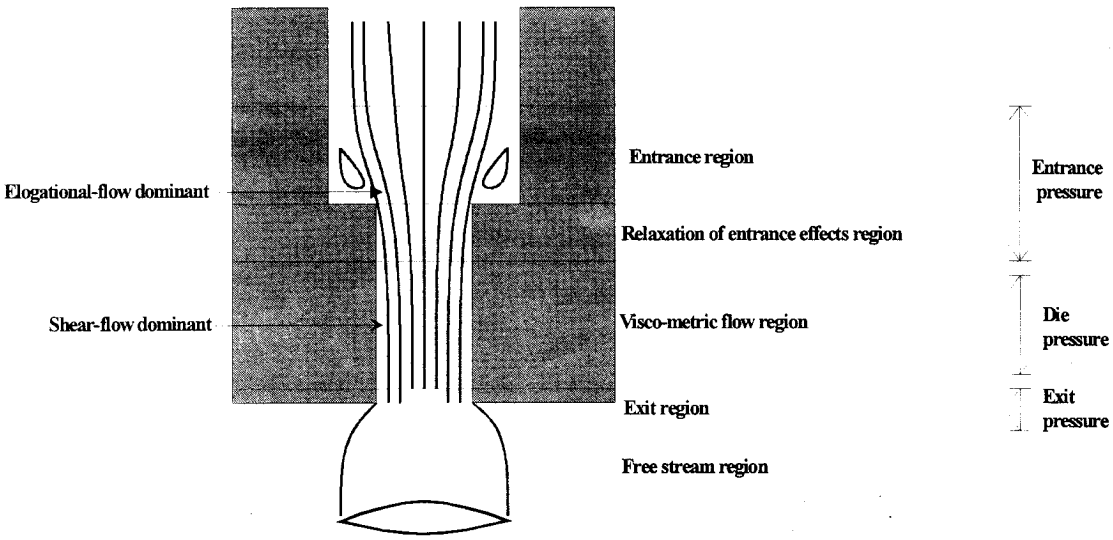

Fig. 1 Five regions of the ideal extrusion die.[1]

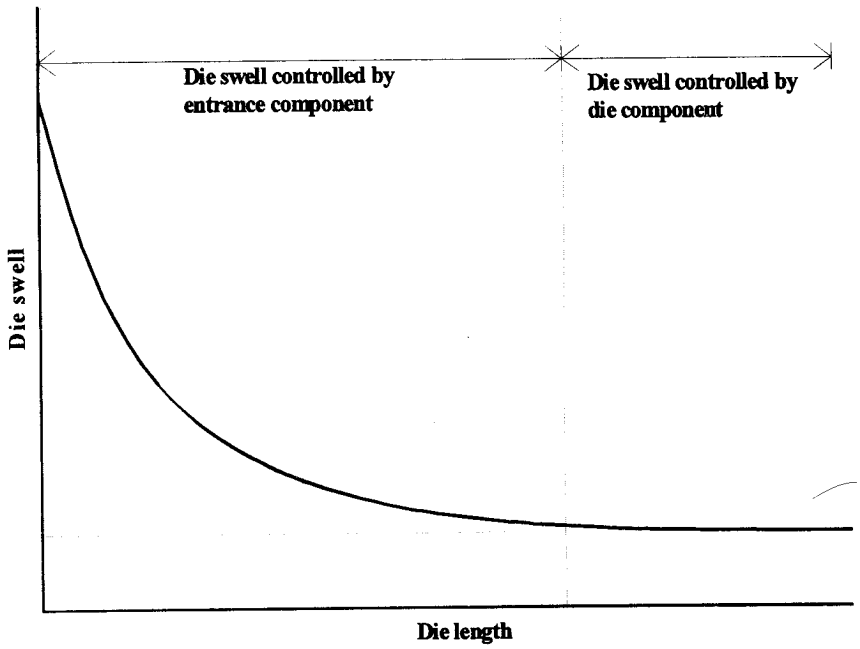

Fig. 2 Effect of die length on extrudate swell.[1]

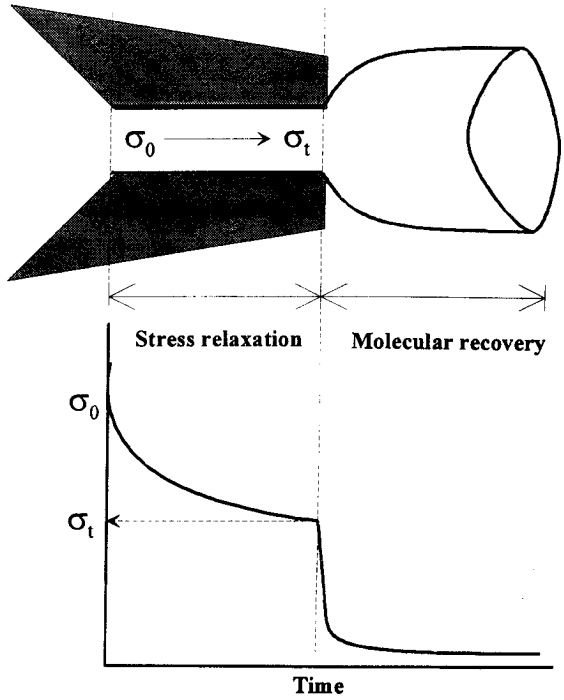

Fig. 3 Stress relaxation and recovery of the extrudate in the die and after emerging from the die lip.

iii) Steady flow region

A combination of steady shear flow and constant pressure gradient are observed in this region.

iv) Exit region

A sudden change in boundary condition occurs in this region and there may be wall slip in the region immediately prior to the exit.

v) Free stream region

A recoverable elastic strain caused by stored elastic energy remaining in the polymer molecules contributes to extrudate swell so as to maximise molecular entropy. As a consequence, the higher the stored elastic energy remaining in the polymer molecules, the higher the extrudate swell will be.

2. BULK RHEOLOGICAL FACTORS AFFECTING EXTRUDATE SWELL

2.1 Stress relaxation

Stress relaxation is the decay in stress with respect to time without any change of geometry. Gent[2] expressed the stress relaxation as a percentage of the initial stress, as illustrated in equation (1).

$$\text{stress relaxation} = \frac{\sigma_0 - \sigma_t}{\sigma_0} \cdot 100 \qquad (1)$$

where σ_0, σ_t = initial stress and stress at time t, respectively.

Generally, there are two types of stress relaxation in polymers: physical and chemical stress relaxations[2-5] but for stress relaxation of extrusion die flow, chemical effects can be disregarded.

The physical stress relaxation is associated with the slippage of molecules passing each other in order to maximise molecular disorder or entropy. It has been reported that the physical stress relaxation rate usually decreases linearly with the logarithm of time, as represented by equation (2)[2]. In addition, the rate of physical stress relaxation is increased by the addition of filler.

$$\frac{\sigma_0 - \sigma_t}{\sigma_0} = A \log\left(\frac{t}{t_0}\right) \tag{2}$$

where A = stress relaxation rate in percent per decade of time (ppd)

Stress relaxation can be characterised approximately by relaxation time (Γ). According to the Maxwell model (Fig. 4), the relaxation time can be quantified using equations (3) and (4).

$$\tau_t = \tau_0 \cdot e^{-\frac{t}{\Gamma}} \tag{3}$$

$$\Gamma = \frac{\eta}{G'} \tag{4}$$

where Γ = relaxation time
τ_t = stored stress at time t
τ_0 = original stored stress
η = viscosity under steady flow
G' = modulus under steady flow

It can clearly be seen from Fig. 5 that the longer the relaxation time, the lower the rate of stress relaxation and thus the greater the elastic response (i.e. the higher the extrudate swell).

Apart from relaxation time, residence time is also a crucial factor governing the elastic response of the extrudate. By definition, the residence time is the time that a polymer melt resides in the die and therefore is proportional to die length. The longer the die, the longer the time for stressed molecules to dissipate their stored energy, and thus the lower the extrudate swell. The average residence time or the so-called transit time (t_{rr}) for a Newtonian fluid can be calculated from equation (5)[6].

$$t_{rr} = \frac{\pi \cdot R^2 L}{Q} = 4 \cdot \left(\frac{L/R}{\dot{\gamma}_w}\right) \tag{5}$$

where L/R = ratio of length to radius
Q = output rate

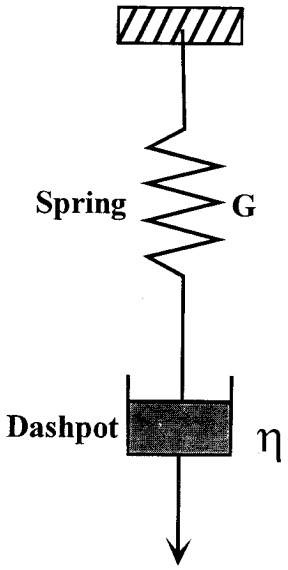

Fig. 4 Mechanical analogue of the Maxwell model.

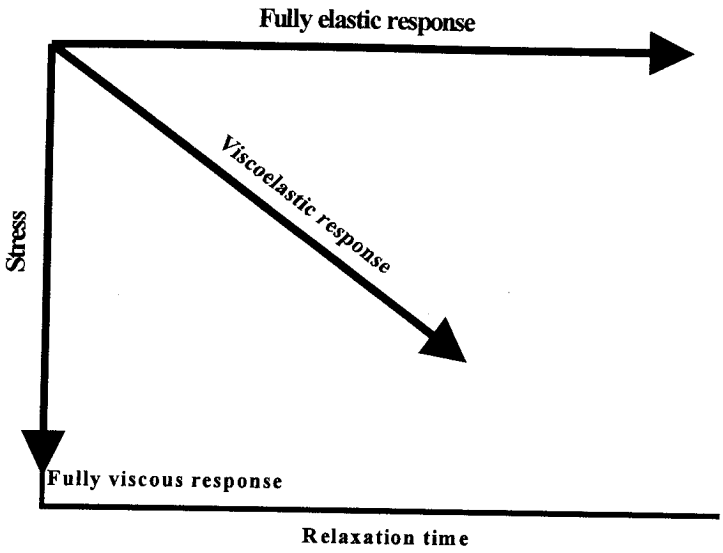

Fig. 5 Stress relaxation of elastic and viscous responses.

Numerous workers have investigated the influence of die geometry on extrudate swell. For example, Bagley *et al.*[7], Aria and Aoyama[8] as well as Huang and White[9] found that extrudate swell decreases as die length increases. Han and Kim[10] reported an increase in extrudate swell with increasing contraction ratio (diameter ratio of reservoir to capillary). Huang and White[9] observed a higher extrudate swell from a slit die than that obtained from a capillary die.

An increase in the extrudate swell of thermoplastics, caused by an increase in shear stress and/or shear rate, has been reported by workers[6, 9]. However, Brydson[11] pointed out that an increase in extrudate swell with increasing shear rate is observed only if the applied shear rate is lower than the critical shear rate. Beyond this point, extrudate swell reduces with increasing shear rate.

Kiriakidis *et al.*[12] proposed that the extrudate swell of linear low density polyethylene (LLDPE) obtained from a long slit die is not affected strongly by shear rate. Many workers[13-14] have observed a decrease in sensitivity of extrudate swell to shear rate and/or shear stress with increasing filler loading.

It has been found that filled and unfilled butadiene-acrylonitrile elastomers (NBR) exhibit only slight increases in extrudate swell as shear rate increases[15]. Additionally, Murty *et al.*[16] observed an independence of extrudate swell on shear rate for a short jute fibre-filled natural rubber compound.

2.2 Recoverable shear strain

It has been reported that extrudate swell increases with the total recoverable shear strain and elastic energy for both thermoplastics and elastomers[17-19]. Consequently, extrudate swell for orifice and long dies can be calculated from recoverable shear strain, as illustrated in equations (6) and (7), respectively[17-18].

$$\varepsilon_r = \ln B_0^2 \tag{6}$$

$$B = \frac{2}{3}\gamma_R \cdot \left[\left(1+\frac{1}{\gamma_R^2}\right)^{\frac{3}{2}} - \frac{1}{\gamma_R^3}\right] \tag{7}$$

$$\gamma_R = \frac{\iota}{G} \tag{8}$$

where B_0, B = extrudate swell obtained from orifice and long dies, respectively
ε_r = recoverable tensile strain
γ_R = recoverable shear strain
τ = shear stress
G = shear modulus

In practice, shear stress can be obtained directly from measured extrusion pressure. Shear modulus can be obtained from the slope of the plot of the Bagley end correction against wall shear stress, as illustrated in equation (9)[20].

$$n_B = n_c + \frac{1}{2}\cdot\left(\frac{\tau_w}{G}\right) \tag{9}$$

where n_B = an imaginary extension of the tube obtained from the Bagley correction
n_c = Couette correction (defined as an elastic geometrical end-correction[21])
τ_w = shear stress at wall
G = shear modulus

2.3 Temperature

The stress relaxation process requires sufficient energy for stressed molecules to overcome the energy barrier for molecular rotation. Consequently, a rise in temperature can increase the rate of stress relaxation, leading to a decrease in extrudate swell. In addition to the increase in rate of stress relaxation, a reduction in viscosity caused by an increase in temperature contributes to a decrease in extrudate swell because of a reduction in stress applied to polymer molecules.

It must be realised that an increase in processing temperature in order to suppress extrudate swell is not an appropriate technique for elastomers, because of the great possibility of scorching. Instead, good die design and compounding formulae should be used.

Nevertheless, the effect of temperature on extrudate swell is very small at shear stresses lower than a critical shear stress. Benyon and Glyde[22] found that the temperature does not strongly affect extrudate swell of polyethylene melts for the whole range of shear stresses.

Yang and Lee[14] investigated the effect of die temperature on extrudate swell under isothermal ($T_{die}=T_{melt}$) and non-isothermal conditions ($T_{die}\neq T_{melt}$). They found that with a long die, differences in extrudate swell obtained under isothermal and non-isothermal conditions were not observed because of a sufficiently long time to reach an equilibrium temperature ($T_{die}=T_{melt}$). By contrast, with a short die, extrudate swell obtained under isothermal and non-isothermal conditions was obviously different due to a lack of thermal equilibrium under the non-isothermal condition.

2.4 Pressure and normal stress difference

Normally, total pressure loss affects extrudate swell through its relationship with shear stress. Therefore, for any given die geometry, the higher the total pressure loss, the higher the extrudate swell[23].

In addition to pressure drop, normal stress difference which can be calculated from pressure drop[24-26] influences extrudate swell. There are many proposed relationships between extrudate swell and normal stress difference. Some of the proposed relationships are shown below:

- Proposed by Racin & Bogue[27]:

$$B=\left\{\frac{\int_0^{\sigma}\left(N_1+G-\frac{\sigma^2}{G}\cdot\sigma\cdot d\sigma\right)}{\int_0^{\sigma}G\sigma\cdot d\sigma}\right\}^{\frac{1}{6}}+0.1 \qquad (10)$$

- Proposed by Anand *et al.*[6]:

$$N_1=2\cdot\tau_w\cdot\left[2\cdot B^6-2\right]^{\frac{1}{2}} \qquad (11)$$

where B = extrudate swell ratio
N_1 = normal stress difference
G = modulus
τ_w, σ = wall shear stress

Apart from the total pressure loss and normal stress difference, entrance pressure also governs the elastic response of extrudate swell. It has been found that the extrudate swell increases with a rise in entrance pressure.[1, 26, 28] The relationship between extrudate swell and entrance pressure for an orifice die has been proposed, as illustrated in equation (12).[28]

$$B = \left[1 + \frac{3}{2}(n+1)k \tan^2 \alpha_0 \frac{\Delta P_{en}}{\tau_w}\right] \tag{12}$$

$$k = \frac{L_e}{D_c} = \frac{e \ln\left(D_p/D\right)}{2\left(D_p/D\right)^{\frac{1}{2}}} \tag{13}$$

$$\tan\alpha_0 = \left(\frac{2\eta_a}{\eta_e}\right)^{\frac{1}{2}} \tag{14}$$

where B = extrudate swell
n = power-law index
ΔP_{en} = entrance pressure loss
τ_w = shear stress at wall
L_e = length of the entrance converging region
η_a, η_e = apparent shear and elongation viscosities, respectively
D_c = diameter of inlet convergence boundary stream-line at $L_e/2$
α_0 = half convergence angle of polymer melts
D_p/D = diameter ratio of the reservoir to die
e = Bagley correction factor

The effect of entrance pressure on extrudate swell fades out with increasing die length because of the longer residence time allowing molecules to dissipate their stored energy[1].

2.5 Molecular characteristics

Although high molecular weight polymers give superior physical properties to low molecular weight polymers, they are difficult to process in practice because of their higher viscosities caused by their greater molecular entanglements. In addition, a large number of molecular entanglements, which act as physical crosslinks[22], contribute to the substantial elasticity of polymer melts, resulting in high extrudate swell.

However, it must be noted that the influence of molecular entanglement on extrudate swell is pronounced only if the molecular weight is higher than the critical molecular weight, which is controlled by molecular stiffness. The stiffer the molecules, the higher the critical molecular weight. In other words, the stiffer molecules require a higher molecular weight for molecular entanglement to affect extrudate swell. Generally, the critical molecular weight is approximately equal to $2M_e$, if M_e is the average molecular weight between entanglement points[29].

Molecular weight distribution (MWD), which can be characterised by the ratio of the weight average molecular weight ($\tilde{M}_w$) to the number average molecular weight ($\tilde{M}_n$), also influences extrudate swell. In the case of narrow molecular weight distribution polymers, all molecular chains have a similar degree of molecular entanglement, leading to uniformly applied

stressing of the molecules during flow. By contrast, in the case of broad-molecular-weight-distribution polymers, the larger chains form a protective network around the shorter chains and therefore, the longer chain molecules are subject to above average stresses.

It has been found that the broad-molecular-weight-distribution polymers show greater elasticity but a slower rate of elastic recovery than do the narrow molecular weight distribution polymers (Fig. 6)[30]. The higher elasticity can be explained by the amount of above average stress applied to the longer molecules. The slower rate of elastic recovery is caused by viscous resistance, due to the conformation of the shorter chain molecules. The shorter chain molecules are initially disentangled and subsequently re-entangled under high stress. As a consequence, during elastic recovery, the re-entangled molecules are compressed and therefore can retard elastic recovery of the system.[23, 30-31]

It is known that the influence of chain branching on flow is significant, particularly for elongational flow, if the molecular weights of branches are greater than the critical molecular weight required for the molecular entanglement. The relaxation rate of branched polymers is significantly lower than that of linear polymers, because the branched polymers cannot freely dissipate the stored energy generated by their resistance to the molecular flow due to their geometry. Therefore, the longer the branches, the longer the relaxation time and thus the greater the extrudate swell. On the other hand, a linear polymer can dissipate stored energy more freely (i.e. shorter relaxation time), leading to lower extrudate swell[23].

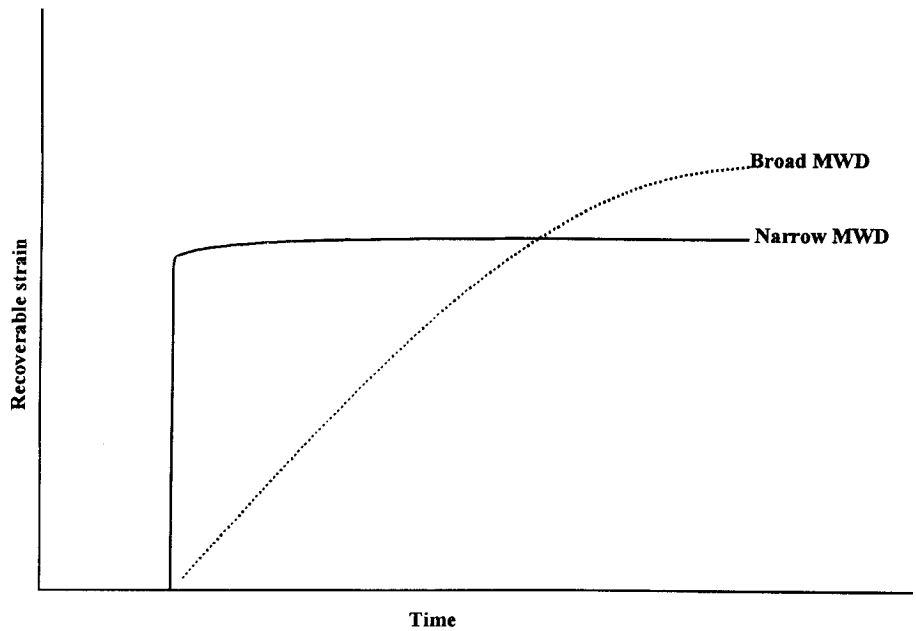

Fig. 6 Effect of molecular weight distribution on recoverable strain.[30]

3. ORIGINS OF EXTRUDATE SWELL IN THE MICROSTRUCTURE OF RUBBER COMPOUNDS

In the practical extrusion process, addition of filler to a compound is necessary because it provides the following advantages:

i) a reduction in production cost (e.g. clay, calcium carbonate)

ii) an improvement in physical properties (e.g. carbon black, silica)

iii) a reduction in extrudate swell

In this section, effects of filler loading, filler-rubber interaction, and addition of additives on extrudate swell will be discussed separately.

Addition of carbon black to raw rubber has been found to reduce the extrudate swell.[23,32-35] The mechanism of reduction in extrudate swell by an addition of filler has been proposed in terms of a dilution effect. Unlike elastomers, the rigid or undeformable filler has no elastic memory. Therefore, filler added to elastomers dilutes the elastic memory, leading to a decrease in extrudate swell[33].

Filler structure (defined as an ability of filler to form agglomerates) and filler particle size can also significantly affect extrudate swell. The higher the structure, the larger the amount of immobilised rubber. The immobilised rubber is assumed to be part of the undeformable filler, which does not have elastic memory and therefore, the larger the amount of immobilised rubber, the lower the elastic memory, resulting in lower extrudate swell[33].

The effect of filler structure on extrudate swell can be characterised by effective volume fraction of filler, as shown in equation (12)[33]. The larger the amount of immobilised rubber, the larger the effective filler volume fraction and hence, the lower the extrudate swell.[33,36]

$$\phi_e = \phi + \phi_{or} \tag{12}$$

where ϕ_e = effective filler volume fraction

ϕ = filler volume fraction

ϕ_{or} = volume fraction of immobilised rubber

It has also been reported that extrudate swell decreases with a decrease in filler particle size.[34, 37-40]

For rubber compounds, filler dispersion is the outstanding factor which controls extrudate swell. It has been proposed that an increase in extrudate swell with increasing filler dispersion is caused by a reduction in effective filler volume fraction, due to the filler disagglomeration.[33, 36, 41-42] However, Pliskin[33] pointed out that although an increase in filler dispersion gives a rise in extrudate swell, the rubber mastication taking place during mixing causes a decrease in molecular weight, resulting in a decrease in extrudate swell. These effects can be seen in Figs. 7a to 7c.

Rubber compounds filled with carbon black loadings higher than 30 phr have been reported to contain a rubber-carbon black tridimensional transient network, which can easily be disrupted by a certain amount of stress.[43-48] This network is expected to decrease extrudate swell because of the increase in energy dissipation[43].

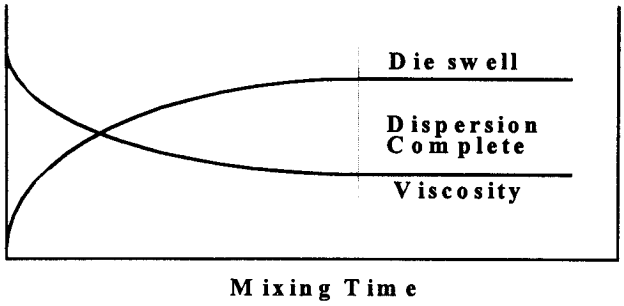

(a)

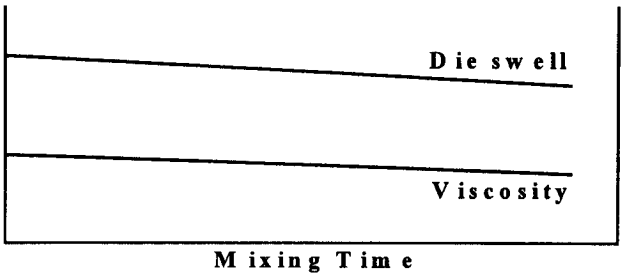

(b)

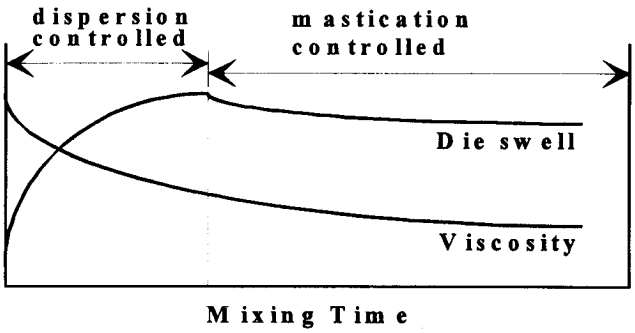

(c)

Fig. 7 (a) Dispersing filler without degrading rubber.[33]

(b) Masticating compound without dispersing filler.[33]

(c) Combined effect of dispersing filler and masticating rubber.[33]

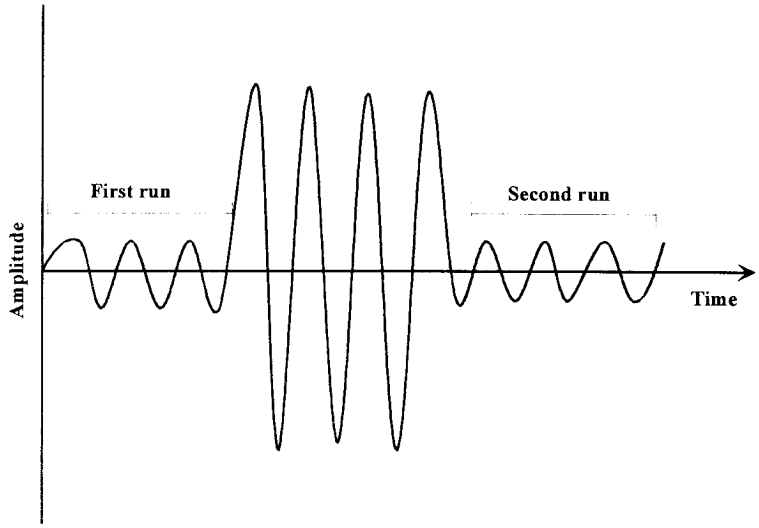

Fig. 8 Strain amplitude applied to samples for rubber-carbon black tridimensional transient network investigation

According to previous work,[44-46] the rubber-carbon black tridimensional transient network can be characterised using the Monsanto Rubber Process Analyser (RPA2000) by applying an alternating sequence of relatively low, high and low strain amplitudes (Fig. 8). Changes in storage moduli are recorded along the whole sequence of strain amplitudes. Theoretically, if the storage moduli measured at low strain amplitude prior to applying the high strain amplitude is higher than that measured after applying the high strain amplitude, the presence of the rubber-carbon black transient network is indicated. By contrast, if there is no significant difference in measured moduli, it illustrates the absence of rubber-carbon black transient network. The concept of the decrease in elastic modulus with increasing strain amplitude due to a disruption of the rubber-carbon black network has been discussed by many workers.[43-46, 48-49]

4. SURFACE AND INTERFACE EFFECTS GOVERNING EXTRUDATE SWELL

4.1 Interaction at polymer/filler interface

It has been proposed that the influence of the polymer/filler interface on extrudate swell is significant in carbon black filled rubber compounds, due to the presence of a rubber-carbon black transient network[5, 15, 35, 50-51]. It is known that this network can be promoted by increasing the surface area and structure of carbon black and by decreasing its particle size[50-51]. The rubber-carbon black transient network is expected to reduce extrudate swell due to the formation of the network in a deformed state, as discussed in the previous section (section 3).

4.2 Slippage at die wall/polymer interface

It is known that steady-state flow in a die is dominated by shear under non-slip condition (pressure-driven flow) and by plug flow under slip condition, as illustrated in Figs. 9a and 9b.

It can be seen from Figs. 9a and 9b that shear stress under the non-slip condition is highest at the die wall and zero at the centre of the die. When slip occurs, the shear stress at the wall, for a given volumetric flow rate, is reduced. Therefore, it is expected that wall slip will reduce extrudate swell because of the lower shear stress applied to

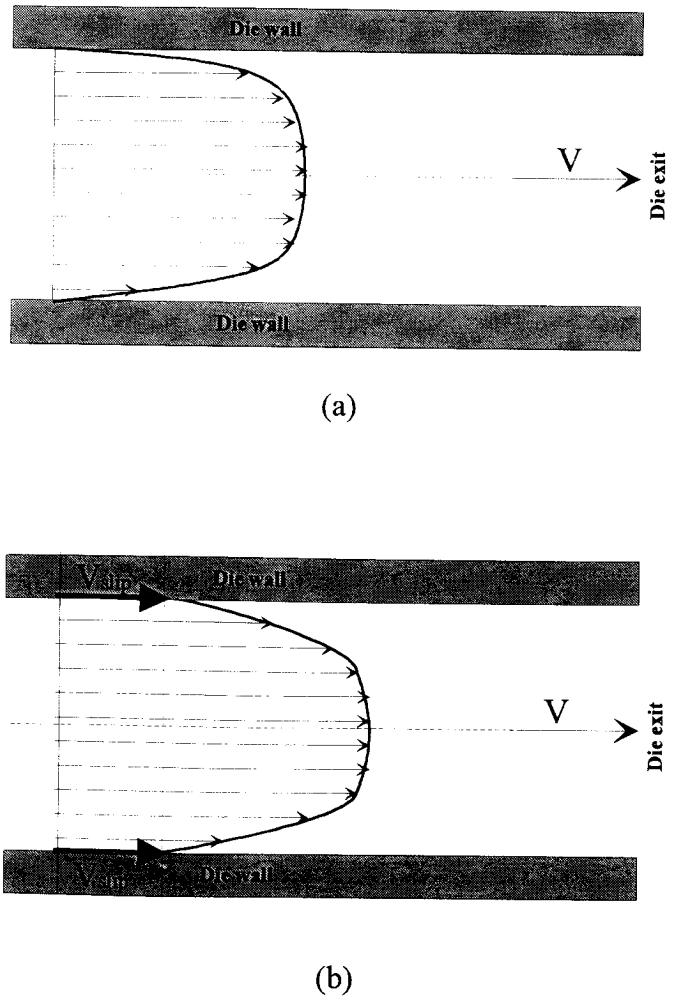

Fig. 9 (a) Flow profile under non-slip condition.
(b) Flow profile under slip condition.

the molecules. It must be noted that the effect of wall slip on extrudate swell will be significant only if the amount of wall slip is large and the onset of wall slip is sufficiently far from the die exit.

So far, there is not much published work on the relationship between extrudate swell and wall slip. Kraynik and Schowalter[52] observed a reduction in extrudate swell of polyvinyl alcohol with increasing wall slip. In contrast, Brzoskowski *et al.*[53] reported that wall slip induced by injecting air pressure between polymer surface and die wall does not significantly influence extrudate swell.

Since wall slip not only affects extrudate swell but also reduces pumping efficiency in the extruder screw channel, the degree of wall slip must be carefully controlled to satisfy the requirement of processability and final products in the practical extrusion process.

Basically, there are two major mechanisms of slippage at the die wall/polymer interface: [1] adhesion failure at the die wall/polymer interface and [2] adhesion failure within the polymer melt near the die wall.

Adhesion failure and lubrication at the die wall/polymer interface

Based on this mechanism, wall slip takes place when applied shear stress is higher than a critical shear stress, which is a function of work of adhesion, when the polymer melt can no longer adhere to the die wall.[54-62]

Factors affecting wall slip based on this proposed mechanism are as follows: hydrostatic pressure, die geometry, temperature, work of adhesion and additives.

It is known that the hydrostatic pressure of shear flow (pressure-driven flow) promotes interfacial adhesion between the die wall and the outer layer of polymer melt. For example, it has been found that the torque of a carbon black filled and unfilled polymer, measured on a rotational rheometer decreases with decreasing pressure due to an increase in wall slip.[30, 55, 57, 60, 63]

It has been reported that the influence of hydrostatic pressure on wall slip in the capillary rheometer is less significant for dies longer than 60D (D is die diameter) because the pressure generated in the dies is sufficiently high to maintain adhesion between polymer and die wall[64].

If the effect of die geometry on wall slip is considered, it can be seen that the effects of die geometry and of pressure are interchangeable. The longer the die, the higher the pressure at a given shear rate and thus the lower the degree of wall slip[64].

Temperature also plays an important role in wall slip. Mälkin *et al.*[65] observed an absence of a critical shear stress at low temperature (70-110 C) for carbon black filled SBR compounds and the slip velocity to be a continuous function of shear stress. By contrast, a critical shear stress is observed at temperatures higher than 110 C and there is no slippage at shear stresses below the critical level. In addition, it has been illustrated that a rise in temperature under slip conditions tends to increase slip velocity.[63-64]

Since the proposed mechanism of wall slip is based on adhesive failure at the polymer/die wall interface, work of adhesion quantified by equation (15) plays an important role in wall slip.[58, 66]

$$W_{ad} = 2 \cdot \left(\gamma_1^d \gamma_2^d\right)^{\frac{1}{2}} \qquad (15)$$

where W_{ad} = work of adhesion

$\gamma_1^d \gamma_2^d$ = surface tensions of polymer and material of die construction, respectively.

It has been observed that an increase in work of adhesion between polymer and die wall contributes to an increase in the critical shear stress.[58, 66] By contrast, Ramamurthy[56] found only a weak dependence of the critical shear stress on materials of die construction.

Hill *et al.*[58] proposed a relationship between the critical shear stress, die geometry and work of adhesion, as shown in equation (16). They mentioned that the critical shear stress increases with work of adhesion but decreases with increasing die radius. In addition, the critical shear stress is not sensitive to temperature due to an insignificant dependence of work of adhesion on temperature.

$$\tau_{wc} \cong \frac{40 W_{ad}}{R} \qquad (16)$$

Generally, there are two major additives which significantly affect wall slip: external lubricating agents and filler. Since the external lubricating agents have low compatibility with the polymer matrix, they tend to migrate to the polymer surface in order to minimise the free energy of molecular interaction between polymer molecules and lubricants. Thereafter, the migrating layers form thin lubricating film between the polymer surface and die wall which promotes wall slip, leading to a reduction in extrusion pressure.[54-55, 60] Surprisingly, Leblanc *et al.*[67] reported the unusual result of an increase in pressure drop due to the lubricating effect.

In addition to external lubricants, fillers can give wall slip in both thermoplastic and elastomeric compounds[35, 68-69]. It has been reported that the minimum filler content, causing wall slip, is 10-15% by weight. Above these loading levels, the degree of slippage increases with increasing filler loading[35].

Adhesive failure within the melt near die wall

According to this mechanism, slippage takes place at the interface between the thin polymer melt film wetting the microscopically rough surface of a die wall, and the main stream flow of the polymer melt[70]. The degree of slippage is controlled by self-adhesion of two layers of polymer melt in close contact through molecular interpenetration. Low molecular weight polymers tend to give lower slippage than do the high molecular weight polymers because of the high level of molecular interpenetration[70].

It has been reported that the low molecular weight species added into the high molecular weight species can act as either plasticisers or slip suppressers, depending on applied shear stress. If the applied shear stress is lower than the critical shear stress, the low molecular weight species act as plasticisers, resulting in a decrease in viscosity. In contrast, if the applied shear stress is higher than the critical shear stress, the low molecular weight species act as slip suppressers instead[70].

5. SLIP VELOCITY

There are numerous methods available to quantify slippage. The classical Mooney technique, as shown in equation (17), has been widely used. By this means, a plot of apparent shear rate against reciprocal die radius is carried out and slip velocity can subsequently be obtained from the slope of the plot divided by four.

$$\frac{4Q}{\pi \cdot R^3} = 4V_s \cdot \frac{1}{R} + \frac{4}{\tau_w^3}\int_{\tau}^{\tau_w} \tau^2 \dot{\gamma} \cdot d\tau \qquad (17)$$

where V_s = slip velocity
Q = output rate
R = die radius
t, t_w = shear stress and shear stress at wall, respectively
$\dot{\gamma}$ = shear rate

Nonetheless, the Mooney technique is not valid for practical conditions because of the following assumptions:

i) wall shear stress, slip velocity and pressure gradient are constant along the die
ii) slip velocity does not depend on die diameter.

There are a number of attempts to modify the classical Mooney technique in order to obtain more accurate values of the slip velocity. For instance, Kalika and Denn[71] investigated wall slip of LLDPE using a capillary rheometer with a long die in order to eliminate the end effect. They proposed an expression for calculating slip velocity, as shown in equation (18). It is necessary to note that this technique is not suitable for elastomeric compounds because their high viscosities result in a tremendous extrusion pressure.

$$\frac{8V}{D} = \frac{8V_s}{D} + \left(\frac{3n}{4n+1}\right)\cdot\left(\frac{\tau_{wp}}{K}\right)^{\frac{1}{n}} \tag{18}$$

where V_s = slip velocity
V = ram speed
n = power law index
t_{wp} = pressure-corrected shear stress
K = consistency constant

Hatzikiriakos and Dealy[64] postulated the calculation of slip velocity, as shown in equation (19). It can be seen that only a single experimental flow curve is required for this method, which is a major advantage over the Mooney technique.

$$\frac{8u_s(z_0)}{D} = \dot{\gamma}_A - \left[\frac{4n}{3n+1}\right]\cdot\left[\frac{\sigma_w(z_0)}{K}\right]^{\frac{1}{n}} \tag{19}$$

where $u_s(z_0)$ = slip velocity at the axial distance z_0
$\sigma_w(z_0)$ = wall shear stress at the axial distance z_0
z_0 = axial distance in the die at which the wall shear stress is equal to $\sigma_w(z_0)$
n = power law index
K = consistency constant

Hatzikiriakos and Dealy[72] also proposed an equation for calculating slip velocity for low-flow-rate and high-flow-rate branches of flow curves in the oscillating flow region, as shown in equations (20) and (21), respectively. Notably, the high-flow branch region of the flow curve is governed by wall slip rather than shear flow, as illustrated in equation (21).

$$u_s = \xi_0\left[\frac{C_1^0(T-T_0)}{C_2^0(T-T_0)}\right]\left(\frac{\sigma_w}{\sigma_{c1}I^{\frac{1}{4}}}\right)^m\left\{1-c_2\tanh\left[\frac{1}{RT}\left(E+c_3\frac{\sigma_n}{\sigma_w}\right)\right]\right\} \tag{20}$$

$$u_s = a\cdot\sigma_w^m \tag{21}$$

where u_s = slip velocity
ξ_0 = empirical constant
σ_{c1} = the first critical shear stress for the onset of slip
σ_w = wall shear stress

m = constant, dependent on type of polymer
C_1^0, C_2^0 = empirical constants that are fitted to the experimental data
c_2, c_3 = empirical constants
T_0, T = absolute reference temperature and temperature T, respectively
R = gas constant
I = polydispersity index

Mourniac *et al.*[61] proposed that the slip velocity of SBR compounds, caused by lubricating layers of additives, can be represented by equations (22) and (23). They also mentioned that the slip velocities of lubricating layers increase with a reduction in die radius because of an increase in the ratio of surface area to volume of flow.

$$V_s = \frac{Q - Q^*}{\pi R^2} \tag{22}$$

$$\tau_w = \alpha \cdot K V_s^n \tag{23}$$

where V_s = slip velocity
Q, Q* = flow rate with and without slip, respectively
α = slip parameter, dependent on materials and die geometry
K = consistency constant
n = power law index

Stewart *et al.*[73] developed a model for predicting slip velocity during extrusion by assuming that slip takes place when the centre of mass of molecules can pass over the potential energy barrier for molecular rotation. The proposed equation is shown in equation (24).

$$u_s = 2 \cdot \left(\frac{\phi kT}{Mh}\right) \exp\left(\frac{-\Delta F^*}{kT}\right) \sinh\left(\frac{\Delta F_w}{kT}\right) \tag{24}$$

$$\Delta F_w = \frac{fM\sigma_w \gamma_{r,s}}{2\rho N} \tag{25}$$

$$\Delta F^* = C' W_{ad} \rho^{-\frac{2}{3}} = C_1 \rho^{\frac{4}{3}} \left(\gamma_d^0 \gamma_p^0\right)^{\frac{1}{2}} \tag{26}$$

where k = Boltzmann constant
σ_w = wall shear stress
T = Absolute temperature
h = Planck's constant
M = molecular weight
ΔF_w = strain energy
ΔF^* = activation free energy

N = normal stress
$\gamma_{r,s}$ = recoverable shear
W_{ad} = work of adhesion
γ_d^0, γ_p^0 = surface tension of the die surface and fluid polymer, respectively
ρ = bulk polymer density
C_1, C' = constants
f = fraction of the stored elastic free energy available to overcome the free energy barrier

Apart from the capillary rheometer, rotational and other rheometers can also be used for quantifying wall slip. For example, Turner and Moore[55] investigated the wall slip of rubber compounds caused by a lubricating layer using the Negretti TMS biconical rotor rheometer. They calculated a slip velocity from the difference between the rotor speeds measured on polished and grooved rotors, as shown in equation (27).

$$V_s = 2\pi \cdot r\left(S_p - S_g\right) \tag{27}$$

where V_s = slip velocity
r = radius of the rotor edge
S_p, S_g = rotor speeds of polished and grooved rotors, respectively

Yoshimura and Prud'homme[74] proposed methods for quantifying wall slip using Couette geometry (using different radii) and parallel disk geometry (using different gap heights), as illustrated in equations (28) and (29), respectively. They claimed that the major advantage of their proposed methods is that only two measurements, instead of at least three measurements in the Mooney technique, are required.

$$u_s = \left(\frac{k}{k+1}\right)\cdot\left(\frac{\Omega_1 - \Omega_2}{\frac{1}{R_1} - \frac{1}{R_2}}\right) \tag{28}$$

$$u_s = \frac{\dot{\gamma}_{a_1} - \dot{\gamma}_{a_2}}{2\cdot\left(\frac{1}{H_1} - \frac{1}{H_2}\right)} \tag{29}$$

where u_s = slip velocity
Ω_1, Ω_2 = angular velocities of the first and second measurements, respectively
R_1, R_2 = bob radii of the first and second measurements, respectively
H_1, H_2 = gap distances of the first and second measurements, respectively
$\dot{\gamma}_{R_1}, \dot{\gamma}_{R_2}$ = shear rates of the first and second measurements, respectively
k = constant

Hatzikiriakos and Dealy[59] studied wall slip of HDPE using a sliding plate rheometer, which has no entrance effect and related pressure gradient, under three conditions: steady, transient, and dynamic shear. Under steady shear, changes in the slopes of flow curves are observed which are assigned to the effect of wall slip. The slip velocity under steady shear can be calculated from the power law equation shown in equation (30). Slip velocity under transient shear can be obtained from equation (31). Under dynamic shear, it was found that the adhesion between polymer molecules and the wall exists only for a certain number of cycles before wall slip takes place. Slip velocity under dynamic shear can be quantified from equation (32).

$$\frac{2u_s}{h} = \dot{\gamma} - \left(\frac{\sigma_w}{K}\right)^n \tag{30}$$

$$u_s = \lambda_s \cdot \left(\frac{du_s}{dt}\right) = a\sigma^m \tag{31}$$

$$\sigma_w + \lambda_s \cdot \left(\frac{d\sigma}{dt}\right) = \eta_0 \cdot \left[\gamma_0 \omega \cos(\omega t) - \frac{2u_s}{h}\right] \tag{32}$$

where u_s = slip velocity
h = gap distance
K = power law coefficient
σ_w = wall shear stress
m = constant, dependent on type of polymer
n = power law index
a = slip coefficient
λ_s = slip relaxation time, weakly dependent on shear stress
γ_0 = nominal strain amplitude
ω = frequency
$\dot{\gamma}$ = shear rate

6. QUANTIFICATION OF EXTRUDATE SWELL

There are a number of ways of measuring extrudate swell. The easiest way is to quench the extrudate in air or liquid before measuring its diameter. It has been found that this conventional method gives the lowest extrudate swell[14]. The second method is to anneal the quenched extrudate in a liquid bath above the glass transition temperature. By this means, the extrudate swell increases due to stress relaxation of the oriented molecules (stressed molecules).[6, 9, 14] The third way is to extrude polymer melts into a heated chamber for molecular relaxation[14]. The fourth method is to extrude polymer melts into an oil bath, whose oil density is very close to the density of polymer melts. Subsequently, extrudate swell is measured using non-contact method such as laser optometry[14]. It has been reported that the fourth method gives higher measured extrudate swell than the annealing method[14].

Although the isothermal method (the fourth method) provides a reasonable measurement of extrudate swell in theory, the disadvantages of this method are the difficulties of mounting the hot oil bath on the rheometer and of matching the oil density to that of the polymer melts[14].

Notably, gravity also plays an important role in an accuracy of extrudate swell measurement and can cause a non-uniform extrudate swell; the larger swell at the bottom and smaller swell at the top. This effect is more noticeable in slow extrusion rate and known as "sagging".

In order to minimise errors in the extrudate swell measurement of thermoplastics, the following measuring conditions should be applied[17]:

i) measured extrudate swell is higher than 1.15
ii) L/D ratio is higher than 16 for a long die but less than 0.1 for a short die
iii) shear rate is lower than 1000 s^{-1}
iv) solidification time is between 5-50 s
v) extrudate diameter is greater than 1 mm
vi) contraction ratio is higher than 5
vii) zero shear viscosity is greater than 10^4 Pa s

In addition to the methods described above, a time-based method has been proposed, as represented by equations (33) and (34)[33]. An important assumption of this method is that the polymer melts are incompressible, i.e. the volume of polymer melt in the die is constant and equal to the volume of extrudate after emerging from the die exit.

$$A'U' = AU \tag{33}$$

$$S = \frac{A'}{A} = \frac{U}{U'} = \frac{U}{\left(d/t\right)} = \left(\frac{U}{d}\right) \cdot t = \text{constant} \cdot t \tag{34}$$

where U = average velocity of the extrudate in the die (dependent on ram speed and die geometry)
U′ = average velocity of the extrudate outside the die
A, A′ = cross-sectional area of the die and extrudate, respectively
d = extrudate length at time t
S = extrudate swell
t = time required to obtain extrudate length d

It can be seen that if the length of extrudate obtained at time t (denoted as d in equation (34)) is adjusted to give a U/d ratio of unity, the time required to obtain the extrudate length "d" is equal to the extrudate swell. Advantages of this method are its precision and simplicity in measurement because extrudate swell is measured at the processing temperature and no external contact, cutting, or weighing are required. Obviously, the disadvantage of this method arises from the difficulty of adjusting the extrudate length in order to yield the ratio of U/d of unity. Additionally, sagging can contribute to a significant error if time t is too long.

It has been reported that the measurement of extrudate swell by measuring extrudate diameter is less suitable to study the effect of filler type on extrudate swell, compared to the result calculated from weight and length of the extrudate[32].

REFERENCES

1. LeBlanc, J.L., (1989), *Prog. Rubber Plast. Technol.*, **5**, 173-198 .
2. Gent, A.N., (1992), "Engineering with rubber", Hanser, Munich .
3. Tobolsky, A.V., (1960), "Properties and Structure of Polymers", John Wiley & Sons, New York.
4. Aklonis, J.J, MacKnight, W.J., and Shen, M., (1972), "Introduction to Polymer viscoelasticity", John Wiley & Sons, New York.
5. Zhang, Y. and Birley, A.W.A, (1992), *Prog. Rubber Plast. Technol.*, **8**, 318-338.
6. Anand, J.S. and Bhardwaj, I.S., (1980), *Rheol. Acta*, **19**, 614-622.
7. Bagley, E.B., Storey, S.H. and West, D.C., (1963), *J. Appl. Polym. Sci.*, **7**, 1661.
8. Ariai, T. and Aoyama, H., (1963), *Trans. Soc. Rheol.*, **7**, 333.
9. Huang, D.C. and White, J.L., (1979), *Polym. Eng. Sci.*, **19**, 609-616.
10. Han, C.D. and Kim, K.U., (1971), *Polym. Eng. Sci.*, **11**, 395.
11. Brydson, J.A., (1981), "Flow properties of polymer melts", 2nd edition, Godwin, London.
12. Kiriakidis, D.G., Park, H.J,. Mitsoulis, E., Vergnes, B. and Agassant, J.F, (1993), *J. Non-Newt. Fluid Mech.*, **47**, 339-356.
13. Lobe, V.M. and White, J.L., (1979), *Polym. Eng. Sci.*, **19**, 617.
14. Yang, B. and Lee, L.J., (1987), *Polym. Eng. Sci.*, **27**, 1088-1094.
15. Nakajima, N. and Collins, D.A., (1975), *Rubber Chem. Technol.*, **48**, 615-622.
16. Murty, V.M., Gupta, B.R. and De, S.K., (1985), *Plast. Rubber Proc. Appl.*, **5**, 307-311.
17. Cogswell, F.N., (1970), *Plast. Polym.*, **38**, 391-394.
18. Cogswell, F.N., (1972), *Polym. Eng. Sci.*, **12**, 64-75.
19. Debnath, S., (1989), *Intern. Polym. Proc.*, **12**, 225-237.
20. Han, C.D. and Charles, M., (1971), *Trans. Soc. Rheol.*, **15**, 371.
21. Collyer, A.A., (1993), "Techniques in rheological measurement", Chapman and Hall, London.
22. Beynon, D.L.T. and Glyde, B.S., (1960), *British Plast.*, **33**, 414.
23. Dealy, J.M. and Wissbrun, K.F., (1990), "Melt rheology and its role in plastic processing: theory and applications" , Van Nostrand Reinhold, New York.
24. Okubo, S. and Hori, Y., (1979), *J. Rheol.*, **23**, 625-649.
25. Whorlow, R.W., (1992), "Rheological techniques", 2nd edition, Elis Horwood.
26. Seriar, M., Guillet, J. and Carrot, C., (1993), *Rheol. Acta*, **32**, 532-538.
27. Racin, R. and Bogue, D.C., (1979), *J. Rheol.*, **23**, 263-280.
28. Liang, J.Z., (1995), *Plast. Rubber Proc. Appl.*, **23**, 93-95.
29. Ferry, J. D., (1980), "Viscoelastic properties of polymers", 3rd edition, John Willey and Sons, New York.
30. Cogswell, F.N., (1981), "Polymer melt of rheology", 1st edition, Godwin, London.
31. Hamed, G.R. and Song, J.H., (1985), *Rubber Chem. Technol.*, **58**, 407-420.
32. Collins, E.A. and Oetzel, J.T., (1970), *Rubber Age*, **102**, 64-69.
33. Pliskin, I., (1973), *Rubber Chem. Technol.*, **46**, 1218-1233.
34. Shin, K.C., White, J.L. and Nakajima, N., (1990), *J. Non-Newt. Fluid Mech.*, **37**, 95.
35. LeBlanc, J. L., (1994), *Prog. Rubber Plast. Technol.*, **10**, 112-129.
36. Nishimura, T. and Kataoka, T., (1984), *Rheol. Acta*, **23**, 401-407.
37. Minagawa, N. and White, J.L., (1976), *J. Appl. Polym. Sci.*, **20**, 501-523.
38. Han, C.D., Sandford, C. and Yup, H.J., (1978), *Polym. Eng. Sci.*, **18**, 849.
39. White, J.L., Czarnecki, L. and Tanaka, H., (1980), *Rubber Chem. Technol.*, **53**, 823.
40. Tanaka, H. and White, J.L., (1980), *Polym. Eng. Sci.*, **20**, 949.
41. Tokita, N. and Pliskin, I., (1973), *Rubber Chem. Technol.*, **46**, 1116.

42. Clarke, J. and Freakley, P.K., (1994), *Rubber Chem. Technol.*, **67**, 945-956.
43. Leblanc, J.L., (1987), *Kautsch. Gummi-Kunstst.*, **40**, 815-819.
44. LeBlanc, J. L., (1995), *Plast. Rubber Comp. Proc. Appl.*, **24**, 241-248.
45. Coran, A.Y. and Donnet, J.B., (1992), *Rubber Chem. Technol.*, **65**, 1016-1041.
46. Dick, J.S. and Pawloski, H.A., (1993), *paper presented at a meeting of the Rubber Division, American Chemical Society,* 18-21 May, Colorado.
47. Osanaiye, G.L., Leonov, A.I. and White, J.L., (1995), *Rubber Chem. Technol.*, **68**, 50-58.
48. Schaefer, R.J., (1995), *Rubber World*, **212**, 16.
49. Payne, A.R. and Whittaker, R.E., (1971), *Rubber Chem. Technol.*, **44**, 440-478.
50. Nakajima, N. and Scobbo, J.J., JR., (1988), *Rubber Chem. Technol.*, **61**, 137-148.
51. Nakajima, N., (1988), *Rubber Chem. Technol.*, **61**, 938-951.
52. Kraynik, A.M. and Schowalter, W.R., (1981), *J. Rheol.*, **25**, 95-114.
53. Brzoskowski, R., White, J.L., Szydljwski, W., Weissert, F.C., Nakajima, N. and Min, K., (1987), *Rubber Chem. Technol.*, **60**, 945-956.
54. Westover, R.F., (1966), *Polym. Eng. Sci.*, **6**, 83-89.
55. Turner, D.M. and Moore, M.D., (1980), *Plast. Rubber: Proc.*, **5**, 81-84.
56. Ramamurthy, A.V., (1986), *J. Rheol.*, **30**, 337-357.
57. Montes, S., White, J.L., Nakajima, N., Weissert, F.C., and Min, K., (1988), *Rubber Chem. Technol.*, **61**, 698-716.
58. Hill, D.A., Hasegawa, T. and Denn, M.M., (1990), *J. Rheol.*, **34**, 891-918.
59. Hatzikiriakos, S.G. and Dealy, J.M., (1991), *J. Rheol.*, **35**, 497-523.
60. White, J.L., Han, M.H., Nakajima, N. and Brzoskowski, R., (1991), *J. Rheol.*, **35**, 167-189.
61. Mourniac, P., Agassant, J.F. and Vergnes, B., (1992), *Rheol. Acta*, **31**, 65-574.
62. Hatzikiriakos, S.G. and Dealy, J.M., (1993), *Intern. Polym. Proc.*, **8**, 36-43.
63. Hatzikiriakos, S.G, (1993), *Intern. Polym. Proc.*, **8**, 135-142.
64. Hatzikiriakos, S.G. and Dealy, J.M., (1992), *J. Rheol.*, **36**, 703-741.
65. Malkin, A.Y., Baranov, A.V. and Vickulenkora, M.E., (1993), *Rheol. Acta*, **32**, 150-155.
66. Hatzikiriakos, S.G., Stewart, C.W. and Dealy, J.M., (1993), *Intern. Polym. Proc.*, **8**, 30-35.
67. LeBlanc, J.L., Villemaire, J.P., Vergness, B. and Agassant, J.F., (1989), *Plast. Rubber Proc. Appl.*, **11**, 53-57.
68. Ma, C.Y., White, J.L,. Weissert, F.C. and Min, K., (1985), *J. Non-Newt. Fluid Mech.*, **17**, 275-287.
69. Ma, C.Y., White, J.L., Weissert, F.C., Isayev, A.I., Nakajima, N. and Min, K., (1985), *Rubber Chem. Technol.*, **58**, 815-829.
70. Blyler, L.L., JR. and Hart, A.C., JR., (1970), *Polym. Eng. Sci.*, **10**, 193-203.
71. Kalika, D.S. and Denn, M.M., (1987), *J. Rheol.*, **31**, 815-834.
72. Hatzikiriakos, S.G. and Dealy, J.M., (1992), *J. Rheol.*, **36**, 845-884.
73. Stewart, C.W., McMinn, R.S. and Stika, K.M., (1993), *J. Reinf. Plast. Comp.*, **12**, 633-641.
74. Yoshimura, A. and Prud'homme, R.K., (1988), *J. Rheol.*, **32**, 53-67.